ADVANCED FUNCTIONAL MATERIALS
www.afm-journal.de

Photo-Insensitive Amorphous Oxide Thin-Film Transistor Integrated with a Plasmonic Filter for Transparent Electronics

Seongpil Chang, Yun Seon Do, Jong-Woo Kim, Bo Yeon Hwang, Jinnil Choi, Byung-Hyun Choi, Yun-Hi Lee, Kyung Cheol Choi, and Byeong-Kwon Ju**

Recently, research interests in amorphous oxide semiconductors (AOSs) as promising electronic materials have increased considerable. AOSs show superior characteristics necessary for electronic devices: high electron mobility, uniform surface due to its amorphous structure, and high transparency in the visible range.[1,2] In particular, amorphous indium-gallium-zinc-oxide (a-IGZO) shows a mobility over 10 $cm^2 V^{-1} s^{-1}$, which is large enough for operating standard displays such as organic light-emitting diodes (OLEDs) and liquid crystal displays (LCDs) with a fast driving scheme.[1] The controllability of charge density in a-IGZO has been investigated by the simple charge trapping model,[3] and a-IGZO also has process compatibility with conventional fabrication systems. These device-favorable features of a-IGZO based applications have led to creating novel electronics as well as alternating conventional silicon-based devices. Since the first thin film transistor (TFT) with a-IGZO,[4] prototypes composed of a-IGZO TFTs have been demonstrated in various types of transparent or flexible devices such as active matrix (AM) OLEDs, AM LCDs, electronic paper, and oscillators.[2,5,6]

Although a-IGZO has been regarded as a promising material for future electronics, the stability of TFTs has to be ensured for more practical use. OLEDs, for example, undergo negative gate bias stress during most of the driving time and transparent devices are exposed to ambient light unavoidably. The stability resulting from electrical stress under light illumination is important since it can deteriorate the switching performances of a-IGZO-based TFTs. It was found that the positive bias illumination stress is insignificant compared to the negative bias illumination stress (NBIS).[7] NBIS has been explained by photo-induced carriers and the state transition,[7–10] but the exact mechanism is under debate. In addition, previous reports to improve the stability from NBIS are still insufficient from a device viewpoint.

Herein we report a more practical use of a-IGZO-based TFTs by adopting plasmonic filters (PFs). Metal structures at the submicron scale demonstrate a unique optical response known as a surface plasmon (SP). A metallic film with two dimensional nanohole arrays shows high transmission at the SP resonance frequency and the optical response related to this resonance phenomenon can be easily designed by the material and geometrical factors. This structural coloring technology using thin metal films is superior in filtering performance compared to the conventional dye-based color filter that experiences degradation by heat and light due to the low chemical stability of the organic-dye material. In addition, thin and quasi-planar structures are advantageous in that they can be easily integrated with other devices. Therefore, PFs have recently been highlighted for use in industrial imaging applications such as CMOS image sensors and displays.[11,12]

With this point of view, we suggest a novel AOS device that has possible applications in transparent electronics, by integrating a-IGZO-TFTs and PFs. A study on NBIS of the suggested a-IGZO-TFTs combined with PFs was performed. Unlike previous work with white or a monochromatic light source, the photosensitivity of a-IGZO-TFTs was investigated with the selectively controlled spectral range of the illumination by the PFs. The suggested TFTs showed extremely improved stability even under a NBIS environment. In addition, compared to the prior AOS TFTs which were equipped with equipped with metal shielding layer to block the light,[13] our suggestion provides not only the spectral selectivity from the light source but also reduces in the loss of transparency. We expect that the photosensitivity subdivided into spectral ranges will provide a practical guideline for designing structures or a fabrication process of transparent devices and enlarge the usage of AOS TFTs.

Optical Characteristics of Plasmonic Filters: One of a prominent optical phenomena of nanohole arrays compared to that of micron scaled structures is extraordinary optical transmission

S. Chang,[+] J.-W. Kim, B. Y. Hwang, Prof. B.-K. Ju
Department of Electrical Engineering
Korea University
Seoul 136–713, Republic of Korea
E-mail: bkju@korea.ac.kr
Y. S. Do,[+] Prof. K. C. Choi
Department of Electrical Engineering
KAIST, Daejeon 305–701, Republic of Korea
E-mail: kyungcc@kaist.ac.kr
Prof. J. Choi
Department of Mechanical Engineering
Hanbat National University
Daejeon 305–719, Republic of Korea
Dr. B.-H. Choi
Electronic Materials and Module Team
Korea Institute of Ceramic Engineering and Technology
Seoul 153–801, Republic of Korea
Prof. Y.-H. Lee
Department of Physics
Korea University
Seoul 136–713, Republic of Korea
[+]These authors contributed equally to this work.

DOI: 10.1002/adfm.201304114

(EOT), which appears as extremely high transmission in the subwavelength regime.[14] In metallic films with nanoholes, SP resonance works mainly on the enhancement of EOT in the visible wavelength range.[14] The spectral response of the metallic nanohole arrays has multiple transmission peaks calculated by Equation (1) that considers the SP resonance and periodic geometry.[16]

$$\lambda_{\max(i,j)} = \frac{a_0}{\sqrt{i^2 + j^2}} \sqrt{\frac{\varepsilon_m \varepsilon_d}{\varepsilon_m + \varepsilon_d}} \quad (1)$$

Here, (i,j) are integers from the reciprocal vectors of the square array with a period, a_0, and ε_m and ε_d are the permittivity of the metal and dielectric, respectively.

The largest value of λ_{max}, which corresponds to (1,0) or (0,1), shows the highest transmission because SPs interact with the external light more vigorously at a lower energy level (or longer wavelength).[18] The spectral position of λ_{max} can be easily tuned by adjusting a_0 under the given materials from Equation (1). Therefore, metallic nanohole arrays have been introduced as color filter applications that show the selectively filtering function at $\lambda_{(1,0)}$ in each spectral response. Previously, we designed plasmonic color filters (PCFs) optimizing their optical characteristics with a combination of LiF and Al and demonstrated the PCFs with laser interference lithography for large area fabrication.[12]

In this work, we propose the use of PFs for photo-insensitive oxide-TFTs. The transmission peak at λ_{max} shows a Fano-resonance shape: the left side of λ_{max} is affected by the Wood's anomaly, a purely geometric effect, and thus remained a constant value whereas the right side of the peak decreases slowly with increasing wavelength.[16] This phenomenon is noticeable when the lifetime of SPs becomes short, that is, the size of the holes is large (see Figure S1 in Supporting Information). For example, in the case of the green filter this right side tail of λ_{max} results in not only a broader full-width half-maximum (FWHM) but also a higher transmission of red light. In this respect, the plasmonic filter with large holes performs as a low-cut filter for cutting off the wavelength region below λ_{min}.

We performed numerical simulations using a finite-difference time-domain method (FDTD solutions, Lumerical Inc., Canada) to design the PFs that have λ_{max} at red and green as described in previous work,[12] but with larger diameter holes. Since ZnO-based materials are generally sensitive to UV and blue light due to their high energy bandgap, we designed the plasmonic filters to cut off blue light: a) PF-G (Green) cutting off the light wavelength below 470 nm and b) PF-R (Red) cutting off light below 580 nm as shown in Figure S2 in Supporting Information.

Figure 1a represents the schematic of the designed PFs. As mentioned above, the cutoff region was determined by adjusting a_0 within the same composition. A 50-nm-thick LiF layer was deposited on a glass substrate. Then a 150-nm-thick layer of Al, that consisted of patterned square-type arrays with a period (a_0) and hole diameters (d), was deposited on the LiF layer where a_0 = 320 nm and d = 220 nm for PF_G and a_0 = 390 nm and d = 260 nm for PF-R. Lastly, a 150 nm of LiF was deposited for high transmission at λ_{max} by matching SP modes

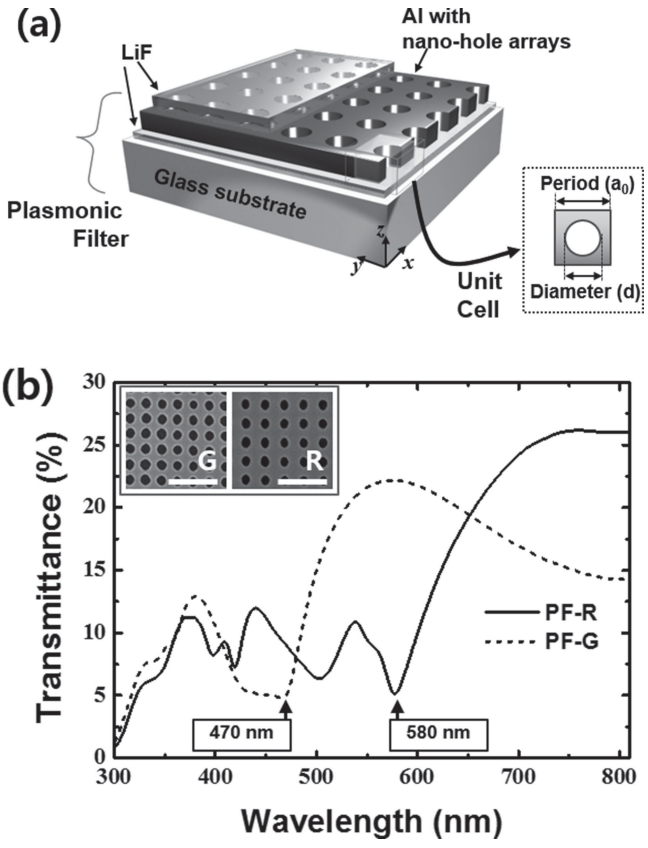

Figure 1. (a) The schematic diagram of the plasmonic filter. (b) The spectral response of the fabricated plasmonic filters. Insets with a scale bar of 1 μm show the scanning electron microscope (SEM) images of the photoresist layers patterned by laser interference lithography. The periods (a_0) of the nanohole arrays were 320 nm and 390 nm for the PF-G and PF-R, respectively.

at two metal-dielectric interfaces.[12] It is also helpful for passivation of the metal surface from oxidization as well as planarization of the structures.

Figure 1b represents the optical characteristics of the fabricated filters. The periodic holes were created by laser interference lithography as shown in the inset images. Although the interference pattern provides good regularity of the periodic domain, the patterned holes in the Al film showed poor uniformity in shape and size and thus resulted in degraded performances compared to the simulation: a) smaller transmittance (22.2% for PF-G and 26.2% for PF-R) and b) broader FWHM.[15] As shown in Figure 1b, the right side tail of λ_{max} showed a much slower decrease rate while the cutoff frequency was in good agreement with the calculations in Figure S1. The broader FWHM resulted in more favorable spectra for low-cut filters.

Enhanced Stability of a-IGZO TFTs under NBIS Using PFs: **Figure 2**a shows the schematic illustration of the suggested TFT integrated with the plasmonic filter. The a-IGZO TFTs with W/L = 40 μm/20 μm were fabricated with a bottom-gate configuration and operated in n-type depletion mode. The electrical properties of the fabricated a-IGZO TFTs were estimated as summarized in Supporting Information

(Figure S3): the saturation mobility (μ_{SAT}) of ~11.9 $cm^2V^{-1}s^{-1}$, the threshold voltage (V_{th}) of –4.74 V, the on/off current ratio ($I_{on/off}$) of 1.39 × 10^7, and the subthreshold gate swing (SS) of 0.39 $Vdec^{-1}$. PFs were attached on the opposite side of the substrate. Since the attached filter screens light with a shorter wavelength than λ_{max} for each filter, the transparent TFTs appeared as different colors as shown in the microscope images in Figure 2b–d.

In order to investigate the device stability under NBIS, we applied the gate/drain stress state with a gate voltage (V_G) of –10 V and drain voltage (V_D) of 10 V for 3000 s under light illumination. A white LED was used as a light source and the intensity during exposure was maintained at 1000 cdm^{-2}.

As expected with general AOS TFTs, as shown in **Figure 3**a, the transfer curve of the reference device (a-IGZO TFT only) showed a negative shift under NBIS. The value of V_{th} for the reference TFT changed from –4.74 V to –6.92 V through 3000 s under NBIS. The deteriorated switching performance, estimated by ΔV_{th}, reduced when the a-IGZO TFTs was integrated with PFs as shown in Figure 3b and c. The NBIS for 3000 s resulted in a ΔV_{th} of –0.58 V for the a-IGZO TFT:PF-G and –0.28 V for the a-IGZO TFT:PF-R.

The negative shift behavior of V_{th} can be explained by the following mechanisms: i) photo-accerlated state-creation from [Vo] to [Vo^{2+}],[10] ii) the hole trapping model,[7] and iii) the oxygen photo-desorption model.[9] We excluded the oxygen desorption effect on account of the passivation on the channel back surface. Other models deal with the variable carrier concentration due to the state transition or photo-created holes that originate from the external light energy. The PF of the suggested device acts as a low-cut filter that blocks the light in the spectral range below λ_{max}. Therefore, the different stability characteristics between the reference and the TFTs integrated with PFs can be simply interpreted by the amount of the variation of photosensitive carriers.

For a more plausible explanation, we investigated the variation of the electric properties of the TFTs during NBIS and their recovery after the stress state, shown **Figure 4**. Figure 4a represents the change in SS for each TFT. All a-IGZO TFTs exhibited comparably stable SS characteristics. It also corresponds that the negative shift of the transfer curves progressed in parallel as shown in Figure 3. SS is obtained by[19]

$$SS = 2.3\frac{kT}{q}\left[1+\frac{C_d + C_{it}}{C_i}\right] \quad (2)$$

where k is the Boltzmann constant, T is absolute temperature, q is the electron charge, and C_i, C_d, and C_{it} are capacitances of the gate, the depletion, and the interface state, respectively. The behavior of SS with changing V_{th} is only affected by C_{it}, which is determined by charge-trapping at the interface between the active layer and the gate-dielectric layer. Thus, the parallel shift

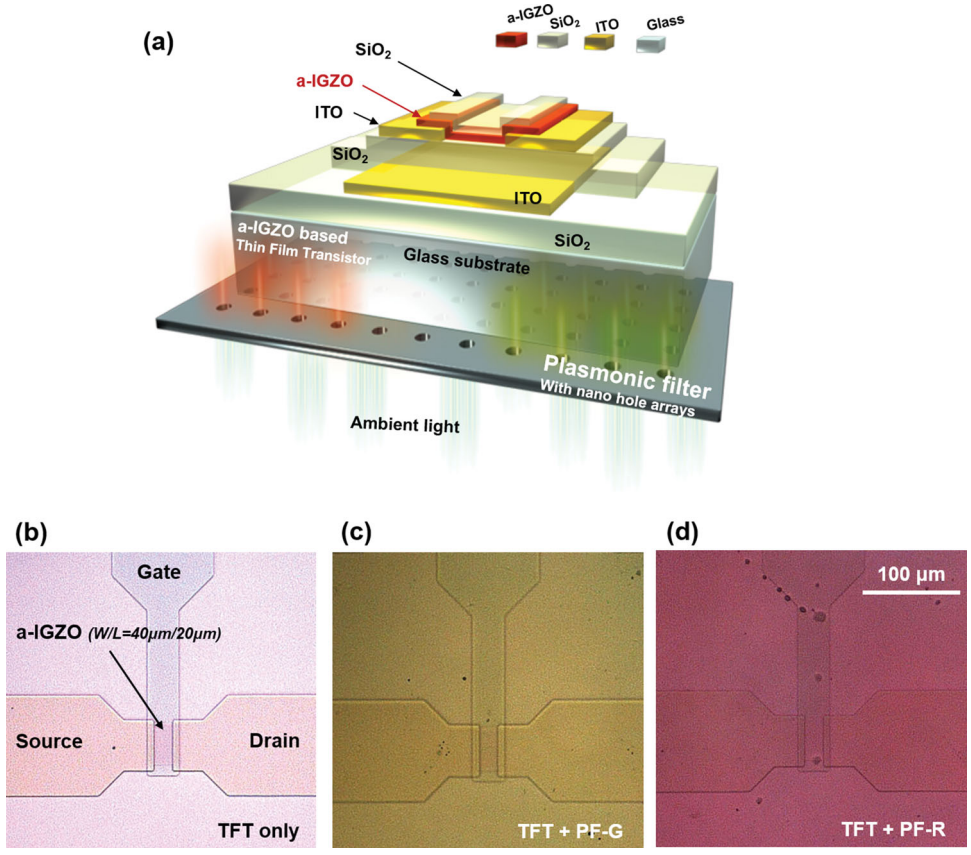

Figure 2. (a) Schematic illustration of the a-IGZO TFT integrated with the plasmonic filter (PF). (b–d) Microscopic image of the fabricated a-IGZO TFTs. The PFs were located at the bottom of the glass substrate: PF-G for (c) and PF-R for (d).

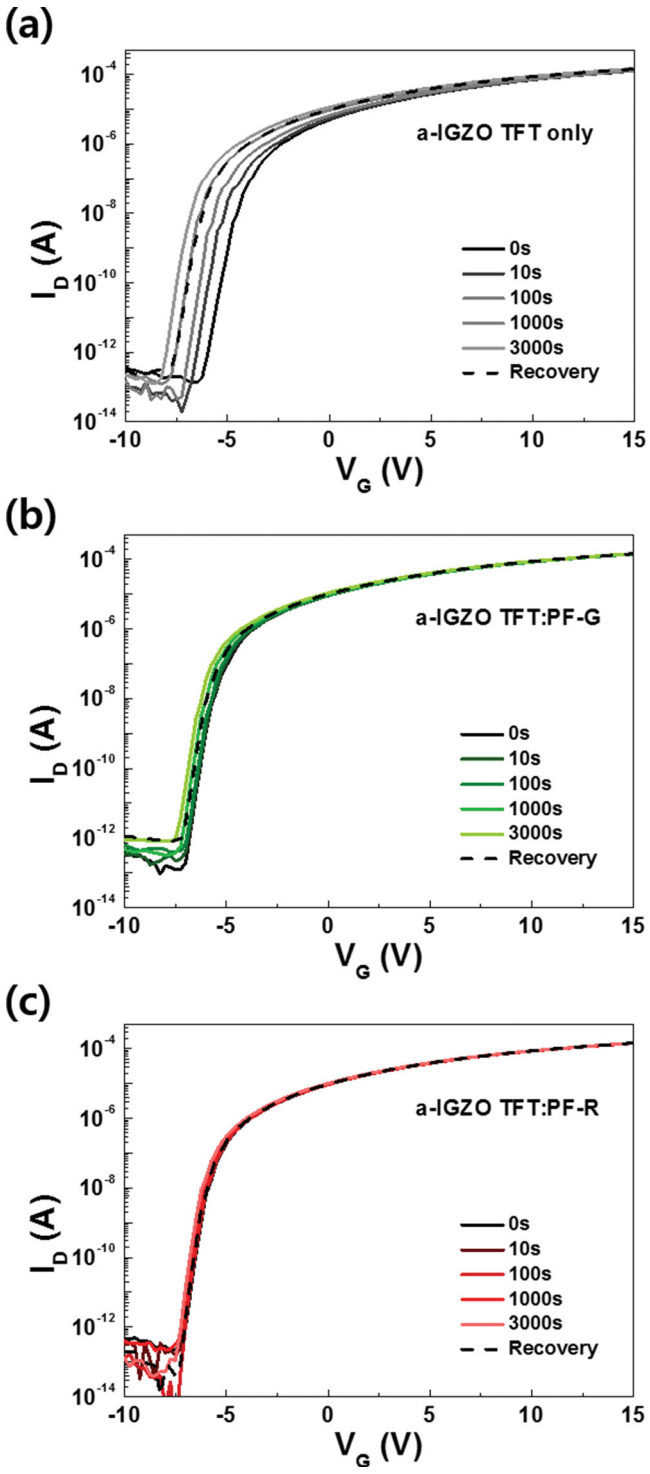

Figure 3. Transfer characteristics of a-IGZO TFTs: (a) the reference TFT without PF, (b) with PF-G, and (c) with PF-R. As increasing λ_{max} of PF, the device characteristics became stabilized via filtered incident light under NBIS condition.

of V_{th} without degradation of *SS* indicates that the charge trapping effects are negligible and the major cause of the V_{th} shift is explained by the photo-created carriers from the oxygen defects.

The external light excites electrons from the ground state [V_O] (~2.5 eV from the conduction band) to the [V_O^{2+}] state (~0.4 eV from the conduction band), releasing delocalized free electrons in the conduction band.[20] In addition, the excited photo-induced electrons from the [V_O] state to the conduction band can be generated.[10] These carriers survive without direct recombination with excess holes that are trapped in the stable [V_O^{2+}] state under NBIS.[8] The released free electrons and [V_O^{2+}] itself lead to the negative shift of V_{th}.

The effect of the photo-created carriers was measured quantitatively with the induced carrier concentration ($\Delta N_d = C_i \Delta V_{th}/qt_{ch}$,[21] where t_{ch} is the channel thickness) as shown in Figure 4b. The N_d of a-IGZO channel was initially estimated to be -3.40 × 10^{17} cm^{-3} and the additional carriers (ΔN_d) with a density of -1.59 × 10^{17} cm^{-3} were generated in the reference TFT throughout the 3000 s under NBIS. After removing the light, the exceeded carriers slightly reduced to –1.15 × 10^{17} cm^{-3} resulting in a V_{th} of –6.3 V. This means that most of the electrons were still in the conduction band. Owing to a thermal barrier (0.2–0.3 eV), the excited [V_O^{2+}] state can also exist after light exposure.[22] Therefore, V_{th} does not recover to its initial condition after NBIS. This behavior causes poor switching properties of the a-IGZO TFTs. Initially, we expected that the PFs could reduce the photo-induced carriers throughout the NBIS duration. This was confirmed by the fact that ΔN_d of the a-IGZO TFTs with PFs appeared much smaller than that of the reference TFT without PF. After 3000 s under NBIS, ΔN_d was found to be -0.39 × 10^{17} cm^{-3} for the a-IGZO:PF-G and –0.23 × 10^{17} cm^{-3} for the a-IGZO:PF-R.

The fabricated PFs had a cut off wavelength of λ_{max}: 470 nm (~2.64 eV) and 580 nm (~2.14 eV) for the PF-G and the PF-R, respectively. Since the transmittance curves of PFs had a slope from λ_{max} to the maximum value, the contrast ratio between the on/off ranges was not exactly distinguished by λ_{max}. Therefore, the energy of the effective spectral range of NBIS in the case of the a-IGZO TFT:PF-G, for example, can be much smaller than 2.64 eV and consequently restrain exciting electrons from [V_O] to [V_O^{2+}] (>2.5 eV). In addition, the downward transmittance (22.2%) reduces the strength of the photo-induced mechanism in the pass band of PFs. Although the energy of the light passing through the PF-G is large enough to make the state transition (>2.1 eV), the amount of electrons in [V_O^{2+}] could decrease. Similarly, the energy within the effective spectral range for the PF-R is smaller than 2.14 eV. This resulted in eliminating both the photo-induced carriers and the state transition.

The results in Figure 3 and Figure 4 indicate that the a-IGZO TFTs are stable in the spectral range greater than 470 nm. This was previously investigated with different wavelength light sources.[5,7,10,17] However, in our current study we investigated the NBIS effect with a white light while tuning the spectral range using PFs. Since the transmission range of nanohole-based PFs is easily tuned via the periodicity of the nanohole arrays, the stability of a-IGZO TFTs with integrated PFs showed potential for more practical use. This is especially true for transparent electronics, components such as the black matrix or color filters can possibly be replaced by PFs to enhance transmission. If a-IGZO TFTs with PCFs are used as imaging devices, the NBIS effect in the deep blue region (<470 nm) should be investigated.

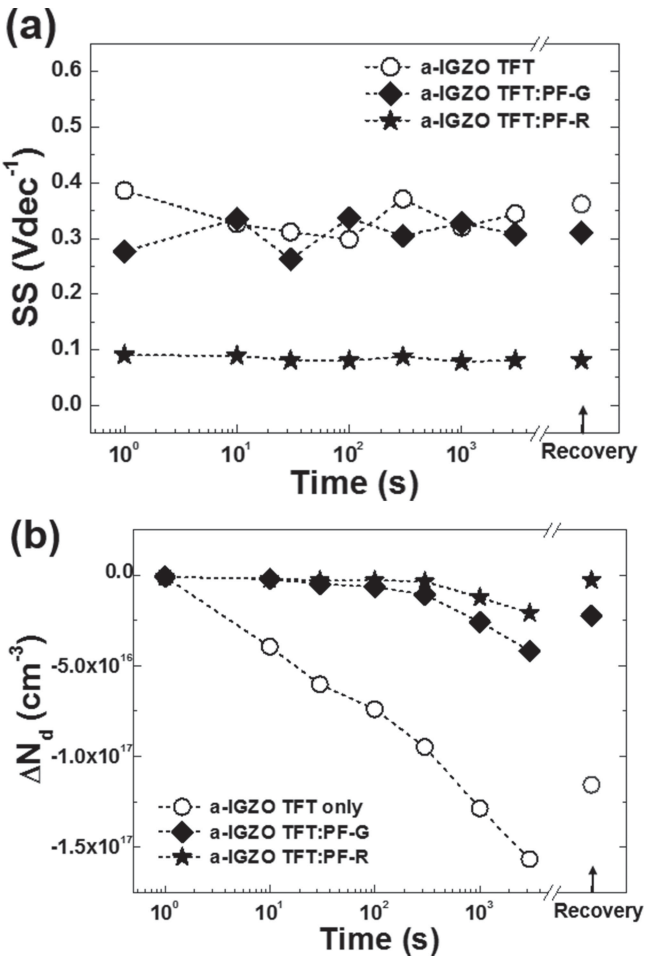

Figure 4. (a) Subthreshold swing (SS) variation and (b) photo-induced carrier concentration of a-IGZO TFTs with species of PFs. SS variation indicated that interface trapping can be negligible thereby all the induced carriers originated from state-transition within the a-IGZO thin film.

In conclusion, we studied photo-insensitive a-IGZO TFTs integrated with PFs. Since the spectral response of PFs is easily controlled, the stability of a-IGZO under NBIS is investigated at different wavelength ranges with a white light source. The PFs block out the light at higher energy, which excites photo-created electrons into the conduction band. In addition, the number of carriers from the state transition of the oxygen defects was restrained by reduced light transmission in the pass band. These results suggest a higher possibility for application to practical devices as well as provide an understandable explanation of the NBIS effect on a-IGZO devices. We believe these results will lead to advances in transparent electronics by giving a realistic guideline to design and fabrication of the AOS-based devices.

Experimental Section

Fabrication of the Plasmonic Filters: In order to pattern nanohole arrays, laser interference lithography was used. A 50-nm-thick LiF film and 150-nm-thick Al film were deposited on a glass substrate by thermal evaporation in sequence. A pretreatment (HMDS:PGMEA = 1.4) was performed for increased adhesion of the photoresist. The photoresist (AR-N4240) mixed with thinner (AR 300–12) at a ratio of 1:1 was spin-coated and resulted in a thickness of 300 nm. The periodic nano patterns were created by a Lloyd's mirror interferometer. Two coherent beams, which were produced from a frequency-doubled argon-ion laser with a wavelength of 257 nm and an output power of 0.16 mW cm^{-2}, formed a 1D interference pattern on the sample for a duration of 140 s. During exposures, the angle between the mirror and the sample (θ) of 30° and 35° corresponded to the length (a_0) of 320 nm and 390 nm, respectively. A successive exposure was performed after a 90° rotation of the sample. After development, a square-type hole array was generated. Next, inductive coupling plasma reactive ion etching (TCP-9600DFM, Lam Research) with chlorine (Cl_2) was performed to pattern holes in the Al film. After removing the photoresist layer, a 150-nm-thick LiF layer was thermally evaporated. Finally, the optical response of the fabricated plasmonic filter was measured by a spectrophotometer (UV-2550, Shimadzu).

Fabrication of a-IGZO Thin Film Transistors: In our experiment, rf-magnetron sputtering was used for depositing ITO and a-IGZO with a deposition pressure of 0.13 Pa in an Ar/O_2 atmosphere (10% O_2). And plasma-enhanced chemical vapor deposition (PECVD) was used for depositing silicon dioxide (SiO_2). A 300-nm-thick SiO_2 buffer layer and 150-nm-thick ITO layer were deposited in sequence on the glass substrate (100 mm × 100 mm). The ITO layer was then deposited and lithographically patterned for the gate electrode. On top of that, a 300-nm-thick SiO_2 layer and 150-nm-thick ITO layer were deposited and the ITO layer was patterned with a wet-process in order to make the source/drain electrodes. Subsequently, a 30-nm-thick a-IGZO active layer and 100-nm-thick SiO_2 passivation layer were deposited in sequence. These two layers were simultaneously patterned by a wet-process. In our devices, the width/length (W/L) ratio was defined as 40 μm/20 μm. After fabrication of a-IGZO TFTs, a thermal annealing process was performed at 300 °C in ambient air for 2 h. The electrical characteristics of a-IGZO TFTs were characterized by using the semiconductor parameter analyzer (Keithley SCS 4200) in a dark-box. A white LED was used as a light source and the light intensity was maintained at 1000 cd/m^2 while measuring the light-induced instability.

Acknowledgements

This research was supported by the National Research Foundation of Korea (NRF) grants funded by the Korea government (MSIP) (CAFDC/Byeong-Kwon Ju and Kyung Cheol Choi/No. 2007–0056090) and (No. 2011–0016621). Also, this work was partially supported by the IT R&D program of MKE/KEIT(Grant No. 10041416, The core technology development of light and space adaptable new mode display for energy saving on 7inch and 2W).

Received: December 8, 2013
Revised: January 12, 2014
Published online: March 17, 2014

[1] T. Kamiya, H. Hosono, *NPG Asia Mater.* **2010**, *2*, 15.
[2] E. Fortunato, P. Barquinha, R. Martins, *Adv. Mater.* **2012**, *24*, 2945.
[3] A. Suresh, J. F. Muth, *Appl. Phys. Lett.* **2008**, *92*, 033502.
[4] K. Nomura, H. Ohta, A. Takagi, T. Kamiya, M. Hirano, H. Hosono, *Nature* **2004**, *432*, 488.
[5] S.-H. K. Park, C.-S. Hwang, M. Ryu, S. Yang, C. Byun, J. Shin, J.-I. Lee, K. Lee, M. S. Oh, S. Im, *Adv. Mater.* **2009**, *21*, 678.
[6] A. Suresh, P. Wellenius, V. Baliga, H. Luo, L. M. Lunardi, J. F. Muth, *IEEE Elec. Dev. Lett.* **2010**, *31*, 317.
[7] J. H. Jeon, J. Kim, M. K. Ryu, *J. Kor. Phys. Soc.* **2011**, *58*, 158.

[8] J. S. Park, T. S. Kim, K. S. Son, J. S. Jung, K. H. Lee, J. Y. Kwon, B. Koo, S. Lee, *IEEE Elec. Dev. Lett.* **2010**, *31*, 440.
[9] a) K.-H. Lee, J. S. Jung, K. S. Son, J. S. Park, T. S. Kim, R. Choi, J. K. Jeong, J.-Y. Kwon, B. Koo, S. Lee, *Appl. Phys. Lett.* **2009**, *95*, 232106; b) T.-C. Chen, T.-C. Chang, T.-Y. Hsieh, C.-T. Tsai, S.-C. Chen, C.-S. Lin, M.-C. Hung, C.-H. Tu, J.-J. Chang, P.-L. Chen, *Appl. Phys. Lett.* **2010**, *97*, 112104.
[10] H. Oh, S. M. Yoon, M. K. Ryu, C. S. Hwang, S. Yang, S. H. K. Park, *Appl. Phys. Lett.* **2010**, *97*, 183502.
[11] a) Q. Chen, D. Chitnis, K. Walls, T. D. Drysdale, S. Collins, D. R. S. Cumming, *IEEE Photonic Tech. Lett.* **2012**, *24*, 197; b) S. Yokogawa, S. P. Burgos, H. A. Atwater, *Nano Lett.* **2012**, *12*, 4349.
[12] Y. S. Do, J. H. Park, B. Y. Hwang, S. M. Lee, B. K. Ju, K. C. Choi, *Adv. Opt. Mater.* **2013**, *1*, 133.
[13] S. Jeon, S.-E. Ahn, I. Song, C. J. Kim, U.-I. Chung, E. Lee, I. Yoo, A. Nathan, S. Lee, J. Robertson, K. Kim, *Nat. Mater.* **2012**, *11*, 301.
[14] T. W. Ebbesen, H. J. Lezec, H. F. Ghaemi, T. Thio, P. A. Wolff, *Nature* **1998**, *391*, 667.
[15] H. T. Liu, P. Lalanne, *Nature* **2008**, *452*, 728.
[16] H. F. Ghaemi, T. Thio, D. E. Grupp, T. W. Ebbesen, H. J. Lezec, *Phys. Rev. B* **1998**, *58*, 6779.
[17] P. Görrn, M. Lehnhardt, T. Riedl, W. Kowalsky, *Appl. Phys. Lett.* **2007**, *91*, 193504.
[18] F. Przybilla, A. Degiron, C. Genet, T. W. Ebbesen, F. de Leon-Perez, J. Bravo-Abad, F. J. Garcia-Vidal, L. Martin-Moreno, *Optic. Express* **2008**, *16*, 9571.
[19] a) D.-C. Hsu, I. Y.-k. Chang, M.-T. Wang, P.-C. Juan, Y. L. Wang, J. Y.-m. Lee, *Appl. Phys. Lett.* **2008**, *92*, 202901; b) M. Huang, I. Mayergoyz, P. Andrei, *J. Appl. Phys.* **2007**, *101*, 014508.
[20] a) B. Ryu, H.-K. Noh, E.-A. Choi, K. J. Chang, *Appl Phys Lett* **2010**, *97*, 022108; b) J. H. Kim, U. K. Kim, Y. J. Chung, C. S. Hwang, *Appl. Phys. Lett.* **2011**, *98*, 232102.
[21] S. Y. Park, J. H. Song, C.-K. Lee, B. G. Son, C.-K. Lee, H. J. Kim, R. Choi, Y. J. Choi, U. K. Kim, C. S. Hwang, *IEEE Electron Dev. Lett.* **2013**, *7*, 894.
[22] A. Janotti, C. G. Van de Walle, *Appl. Phys. Lett.* **2005**, *87*, 122102; S. Lany, A. Zunger, *Phys. Rev. B* **2005**, *72*, 035215.